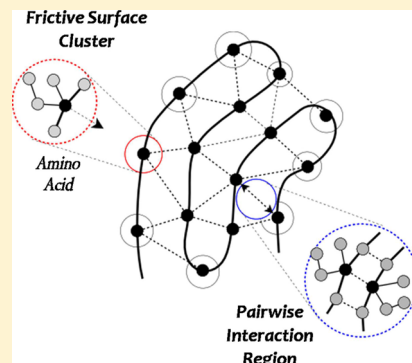


Overdamped Dynamics of Folded Protein Domains within a Locally Harmonic Basin Using Coarse Graining Based on a Partition of Compact Flexible Clusters

Anthony C. Manson and Rob D. Coalson*

Department of Chemistry, University of Pittsburgh, Pittsburgh, Pennsylvania 15260, United States

ABSTRACT: A coarse-graining method based on the partitioning of atoms into compact flexible clusters is used to formulate the dynamics of the nonequilibrium response of a protein to ligand dissociation. The α -carbon positions are used as the degrees of freedom. The net stiffness between each pair of neighboring α -carbons is calculated for the quasi-static, overdamped regime within the harmonic (quadratic potential energy surface) using the equivalent stiffness matrix of the network of atoms occupying the intervening space within the locally interacting region. This localized approach realizes a divide and conquer strategy that results in a substantial reduction in computational complexity while accurately predicting relaxations under general loading conditions. A close correlation between the shapes and time scales of the relaxation curves of the coarse-grained and all-atom instances of two medium-sized proteins, T4 lysozyme and ferric binding protein (each of which having known apo and holo structures), was observed for the holo to the apo transitions. Furthermore, for both proteins the dominant modes of motion and the decay rates of the temporal relaxation profiles monitoring the separation distance between select amino acid pairs were found to be nearly identical when calculated on the coarse-grained and all-atom scales.



■ SECTION 1: INTRODUCTION

The biological functions of proteins are controlled by their cooperative motions, which typically involve the movement of large structural regions.¹ Protein conformational transformations induced by externally applied perturbations, such as ligand binding, are of great biological importance.² Introducing a ligand molecule into a binding pocket induces forces on the protein, causing it to deform in ways that have direct functional implications. Specific types of ligand binding include: (i) binding of agonist molecules, (ii) binding of molecules used for transport and storage, and (iii) binding of drug molecules sufficient to induce conformational changes that can modulate biological function.³ The general description of these complex processes has been impaired by the high intrinsic dimensionality of these systems.

A variety of spatial coarse-graining schemes have been proposed to reduce the dimensionality of large biomolecules and speed up dynamics simulations.⁴ The combination of smaller groups or clusters into larger more massive components can filter out the higher frequency motions within a system.⁵ Examples include 1,2,4,6 bead models.⁶ The reformulated equations of motion for these reduced dimensional models can then be used to determine useful dynamical properties of the system such as (1) vibrational normal modes and (2) nonequilibrium response trajectories.^{7,8}

Atomistic Rigidity Studies. Rigidity has been proposed as a means of limiting the spatial dimensionality of the motion of a macromolecule. Previous atomistic studies describe a rigid body fit of helix and side-chain assemblies to the underlying all-atom

MD trajectory data.⁹ It was found that a rigid body fit to the trajectory data showed high correlation to the atomic fluctuations, especially for the backbone atoms. Even though this suggests that these structures are rigid, it does not mean that they will necessarily remain rigid under an arbitrary applied force. In a previous paper,¹⁰ we attempted to model rigid units and to incorporate these units into the dynamics of the system. We found that even though the motions were qualitatively similar to those of the all-atom control (i.e., the same system with no rigidity constraints imposed), the potential energy surface (PES) was steeper than the all-atom control so the relaxations of the Langevin modes were faster. This was a consequence of the lack of energy storage in the rigid structures. The approach proposed in the current paper is designed to fix the condition where the internal stiffness of rigid clusters is similar to that of the intercluster stiffness, a condition common in proteins.

In our previous study of rigid block dynamics,¹⁰ which did not allow for internal distortions within a block, we suggested two ways to rectify the problems associated with purely rigid blocking. One way is to add back a subset of the suppressed internal (vibrational) degrees of freedom in each block to the six rotation-translation block (RTB) degrees of freedom (dof's). In principle, if the blocks are large and if the number of internal vibrational modes needed to represent the

Received: February 18, 2013

Revised: May 2, 2013

conformational changes in the protein that are of interest is modest, this could result in a significant reduction in the relevant degrees of freedom. However, under general loading conditions, it is difficult to anticipate *a priori* which degrees of vibrational motion will be important in a given fragment and to guarantee that the number of such dof's will be small. A second possible approach is to reduce the effective spring constants that couple pairs of blocks to reduce artificial energy strains induced by the RTB procedure. In the present work, we propose a solution of the second type, which is computationally efficient and in numerical tests proves to be accurate for studying ligand-induced conformational changes in globular proteins immersed in water.

Related Work. A multiscale modeling approach, where different parts of the molecule are modeled at different levels of detail, can be achieved by substructuring, where the molecular system is partitioned by collecting groups of atoms into rigid or flexible bodies. Molecular flexibility is typically modeled by a truncated set of low-frequency all-atom normal modes that allow for the elimination of the high-frequency harmonic motion.¹¹

Because the dominant motion of a protein structure occurs along the polymer backbone (due to the stiff covalent bonds), one can simplify the potential field of the protein structure by using the α -carbon atoms. This has proven to be useful in the coarse-grained (CG) modeling of proteins. Here the decomposition of a large assembly of units can be modeled as a network of many discrete units connected by several kinds of typically pairwise interactions that are modeled as generalized springs with varying force constants.¹² Such force constants have been calculated from the variance-covariance matrix obtained from atomistic molecular dynamics (MD) simulation.¹³ Although it is tempting to approximate a system with a single spring constant, it has been found that the conformational motion of molecules modeled with single force constant springs does not always correspond well to analogous motion predicted by full force field molecular mechanical models. In particular, it has been observed that the unimodal density of vibrational mode frequency distribution obtained using the uniform spring constant elastic network model (ENM)¹⁴ disagrees with the bimodal distribution obtained from all-atom models.¹⁵ It has further been found that such a bimodal distribution can be recovered by strengthening interactions between atoms that are backbone neighbors.¹⁵

Elastic network models do not take full cognizance of the molecular level energetics that give rise to the protein's structure and function. They replace the actual intramolecular force field (or, equivalently, PES) with a network of generic springs that couple, indiscriminately, pairs of protein atoms that lie within a certain proximity of each other. In particular, the ENM force field does not yield accurate estimates of the eigenvalues of the normal modes of the protein and hence cannot be used to predict time scales of large-scale conformational motions, which are generally realized as a linear combination of several cooperative normal modes. In addition, standard ENM methodology treats the motion of the isolated protein; that is, it does not include frictional damping and thermal agitation associated with the solvent. In contrast, the technique outlined in the paper uses the underlying all-atom force field (based on quantum chemistry and molecular spectroscopy) to derive an estimate of the CG interactions. Furthermore, the critical influence of the water solvent on the protein motion is included at the Langevin equation level. In

addition to providing more accurate energetics of the underlying modes, this will properly represent motions that will not be captured in traditional ENM.

A key advantage of expressing the protein motion in terms of Langevin normal modes is that they provide a compact understanding of the system. Direct analysis using MD simulations gives more complete information but can bury the problem and make a summary understanding more difficult. In the current analysis, the overall cooperative process can be understood in terms of a small number of Langevin modes and their time decay coefficients. We focus our numerical illustrations in the present work on modest-sized proteins (150–300 residues) for the sake of conceptual clarity. Although such systems, if desired, could be analyzed at a higher level of realism via MD simulation, it is reasonable to expect that there will be larger protein systems for which current MD hardware would require an excessive simulation time-scale, while the CG harmonic oscillator Langevin model could still be applied. (Gating motions in multisubunit ion channel proteins¹⁶ provide one example where the utility of MD is at present limited,^{17,18} while the Langevin mode model presented here could be implemented without excessive difficulty.)

Current Work. The following issues in the collective mode analysis of compact protein domains have been identified. (1) Using the all-atom Hessian can result in excessive time and space complexity, especially while calculating the normal modes.¹⁹ (2) Assigning a uniform stiffness between CG elements can result in improperly shaped modes of motion that fail to reproduce biologically relevant motion.²⁰ (3) The application of rigid blocking can artificially steepen the PES.¹⁰

To remedy these issues, we have developed a tractable coarse-graining method which decomposes a protein into intrinsically flexible clusters (fc's) that will accurately describe the slowest overdamped collective motions. The proposed protocol produces a down-sampled version of the all-atom Hessian matrix such that the overdamped Langevin dynamics of the system (to be denoted here as Brownian dynamics²¹) is found in nontrivial test cases to correlate well with the dynamics and kinematics of the all-atom control (where the motion of all atoms is time-evolved subject to the Hessian of the corresponding all-atom force field).

Outline of Paper. First, we will motivate and then formulate an algorithm that can rescale the all-atom Hessian matrix to accurately capture the slow Brownian modes (BrM) that govern protein conformational motion. Second, we will assess the viability of the method by studying select protein systems from the point of view of their cooperative relaxational motions, comparing these motions to those of the corresponding all atom counterpart.

■ SECTION 2: BASIC THEORY

The purpose of this analysis is to find an efficient and accurate approximation to the all-atom potential interactions for the most collective motions of a folded protein. We will develop here a CG model that essentially tracks the motion of all C_α atoms in the protein. These C_α atoms (each of which can be thought of as representing a cluster of atoms corresponding to the associated residue) are linked energetically by effective harmonic springs and subjected to Brownian motion. To deduce the effective force constant connecting two C_α atoms, we first identify (using tessellation methods described below) a network of intervening protein atoms that directly links the two C_α atoms in question. We then formulate a CG force constant

matrix utilizing a down-sampling approach starting from the all-atom Hessian matrix obtained using an atomistic force field at the energetic minimum of the open conformation. Each CG pairwise interaction force constant is estimated from a statics-based analysis of the displacement of one CG cluster center (C_α atom) under a unit load (applied external force) while the other center is held fixed. The estimated CG force constants are subsequently assembled into the molecular CG force matrix. An appropriate measure of the effective friction constant governing the motion of each cluster is also specified. Time evolution of the C_α (or residue level) motions can then be calculated. As part of this analysis, the small eigenvalue overdamped modes of this system (analogous to low-frequency modes in ordinary vibrational normal mode theory) can be computed and the displacement shapes and time scales compared to the all-atom counterpart.

Motivation for Flexible Cluster Formulation. Because the surface of the molecule interacts with the solvent, the dominant friction effects will be concentrated there (Figure 1)

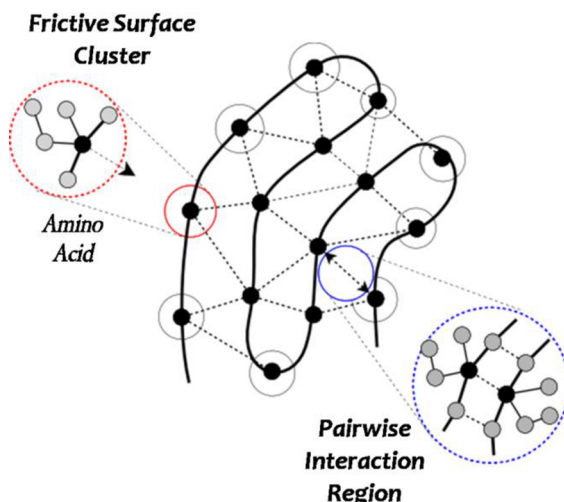


Figure 1. Schematic 2D depiction of a protein molecule having solvent-exposed surface: Small black circles represent α -carbon cluster centers. Strong interactions occur along peptide backbone (solid curved lines) and weaker noncovalent interactions (normal to the backbone) are shown as dashed lines. Secondary (small white) circles represent frictive clusters that are exposed to solvent. The size of each secondary circle indicates the level of friction on each cluster. Atoms residing in internal clusters are assigned a small friction constant to allow for inversion of the friction matrix. The red inset (left) shows atoms of an amino acid that are covalently connected to the α -carbon cluster center. The blue inset (right) shows the region between the α -carbon cluster centers used to compute the effective cluster pairwise stiffness.

for the more collective motions. In contrast, the internal motions of the motion (beneath the solvent surface) will experience less frictional damping and will tend to relax on a faster time scale. These internal motions will result in relatively rapid adjustments that will maintain a state of quasi-equilibrium relative to the time-scale of the overall (collective) motion of the protein (Figure 1). In the present analysis, each fc will correspond to a single amino acid residue within the protein with the dof of the cluster centered at the α -carbon. Because of the covalent links between the atoms of a given cluster member, this assignment will ensure that each cluster will

approximately move as a unit on the time scale of the overdamped relaxation of the entire protein molecule.

Purely rigid blocking can bias the PES by inducing excessive spring displacements in nonblocked regions. This effect becomes more pronounced if the stiffness within the interblock regions is comparable to that of the adjacent intrablock stiffness.¹⁰ This becomes a problem in compact folded protein domains because the covalent bond of the backbone threads through the region in a pseudorandom fashion. If regions containing these covalent bonds are deformed, the harmonic (spring) energy will concentrate in the stiff interblock regions (due to the putative block rigidity) instead of being evenly distributed.¹⁰ To remedy this problem, one must impart flexibility within each block/cluster.

In contrast with more traditional ENM approaches¹⁴ in which a uniform force constant is imparted to each interacting pair of α -carbons, we will estimate the stiffness of the intervening regions between the α -carbon pairs from the all-atom Hessian calculated from the Amber force field.²² This force field pertains to the protein in vacuum. (In our treatment, we will include solvent influence on the motion of the protein via a Langevin equation, in which solvent effects are incorporated by an additional frictional damping force and random force on each atom.) It can be readily appreciated (cf. Figure 2) that due to the presence of the covalent backbone

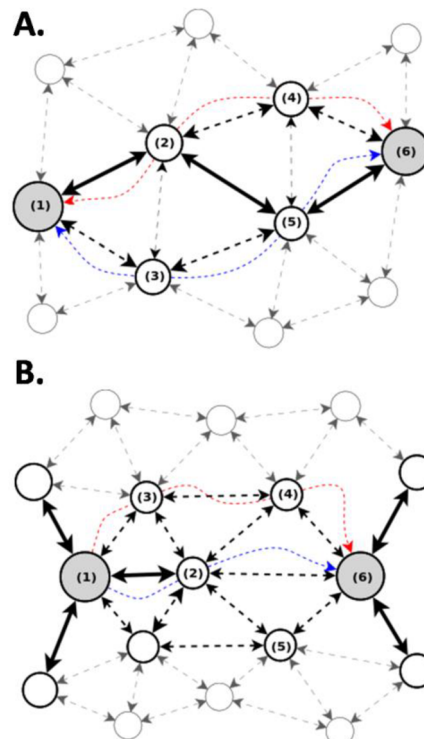


Figure 2. Two representative spring networks used in calculating the effective force constant between neighboring α -carbon positions. (A) Spring network along peptide backbone. (B) Spring network normal to peptide backbone. The heavy solid lines denote covalent (strong) bonds, while the lighter dashed lines denote noncovalent interactions between atoms. The larger gray spheres are the α -carbon centers. For each configuration, two representative paths that partially transmit force from one cluster to the other (dotted spline segments) are shown in red and blue. The linear algebraic procedure discussed in the text calculates the effective force constant due to the aggregate contribution of all such paths.

and side chains the stiffness will be highly anisotropic. To yield correct dynamics, the effective stiffness due to the intervening network of atoms must be systematically determined. In the present analysis we will focus on the regime of overdamped motion, in which the overall motion is limited by solvent friction on the molecule surface.¹⁰

Complexity Reduction. Grouping atoms within a protein will reduce the time and space complexity of a calculation. For instance, diagonalizing the force matrix of an n -atom molecule has a time complexity proportional to n^3 , so reducing the size of the system by a factor of 10 (about the number of atoms in an amino acid) will have a 10^3 fold impact on the time complexity. To further make the calculation of the CG stiffness matrix tractable, we employ a divide and conquer strategy in its formulation. Because the dominant forces that transmit load within the molecule act in a localized fashion (e.g., through covalent and hydrogen bonds), we can approximate the molecule-level force-constant matrix by using these localized stiffnesses and assembling their contributions to construct the CG version of the force matrix. Evaluating these nearest-neighbor stiffness components entails a lower complexity calculation because the number of atoms involved in the cluster pair is much less than the molecule as a whole. This calculation will produce the neighboring cluster to cluster stiffness terms. By applying constraints at the global level, we can calculate the remaining diagonal terms within the CG version of the force matrix (see below).

Stiffness (Force Constant) Matrix Formulation in Terms of Flexible Clusters. In this formulation, the aggregate cluster friction (obtained by summing the atomic frictions within the amino-acid cluster) will be imparted only to the (cluster center) α -carbon. In the calculation of the CG stiffnesses, we will assume that the friction on the intervening atoms between a pair of cluster centers is negligible. These conditions will effectively induce a state of quasi-static equilibrium for the intervening atoms. This is based on the feature of small friction constants for internal atoms in the protein, which enables them to instantaneously adjust to achieve mechanical equilibrium throughout the protein conformational relaxation process.

To compute the molecular response in the overdamped regime, it is necessary to recalculate the force matrix under conditions of cluster-to-cluster quasi-static equilibrium. This requires finding the effective stiffness between the center of a given cluster and each of the neighboring clusters with which it interacts. A Delaunay tessellation²³ in conjunction with its dual (Voronoi) tessellation²³ (Figure 3) is used to determine the region of effective interaction between a CG (α -carbon, α -carbon) pair. The Delaunay tessellation is constructed first using the α -carbon positions as the input nodes.²³ From this, the dual (voronoi) tessellation is constructed.²³ One such region is highlighted in Figure 3A, where it is clear that these regions form a partition in space. The network of atoms participating in each pairwise cluster–cluster interaction (see Figure 3) will select a subset of interactions from the molecular force matrix. The region shown in Figure 3A delineates the boundary of the interaction network for the situation where both cluster centers are buried, that is, beneath the protein surface. Similarly, the region in Figure 3B delineates the boundary when one of the cluster centers occurs on the surface. Such a partitioning scheme will ensure that there is no double-counting of interactions. To illustrate the fine structure within each of these regions, two example interaction networks are

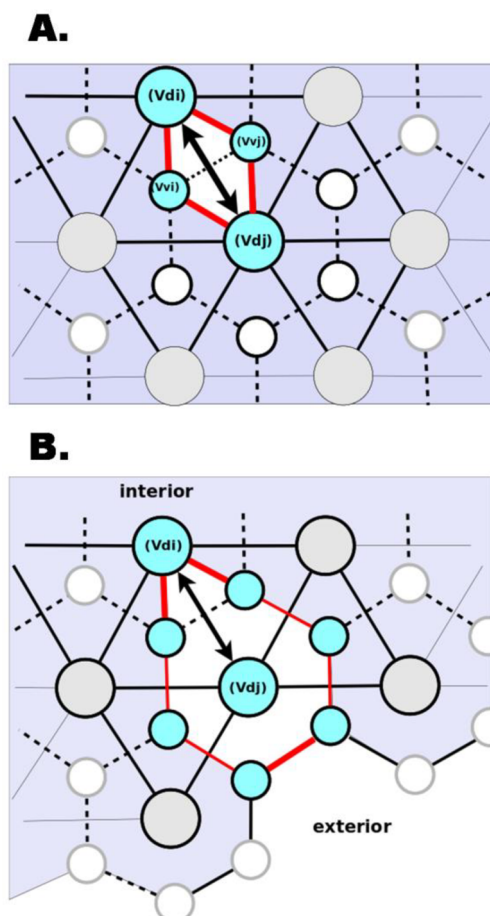


Figure 3. (A) Delineation of the region used to derive the effective, coarse-grained, element stiffness between two adjacent cluster centers: Shown is the Delaunay tessellation using α -carbons as Delaunay vertices (larger circles (labeled: Vd_i), and the principle direction of interaction along the Delaunay edges (solid lines), and the dual (voronoi) tessellation (Voronoi vertices: smaller circles (labeled: Vvi), Voronoi edges: dashed lines). One region delimiting the effective pairwise α -carbon (α -carbon) to α -carbon spring element is highlighted. This effective spring element is formed (by the network of atom–atom interactions) around the Delaunay edge (double arrow connecting adjacent α -carbons) and bounded by Voronoi faces (delimited by smaller cyan circles and red Voronoi edges) that encircle the Delaunay edge. The effective stiffness between α -carbons is derived from the network of atom-level interactions within this region (see text). (B) Similar to panel A except for coarse-grained elements at the molecule boundary. The darker region is the protein interior and the light region is the exterior. The region used to calculate the network of atomic interactions is enlarged for the α -carbon that borders the surface.

shown in Figure 2. Figure 2A depicts the interaction network when both cluster centers occur along the backbone while Figure 2B shows the more general (cross backbone) interaction.

In the following derivations, the indices i and j will refer to atoms, k will refer to one of the three dimensions, and α and β will refer to clusters. The notation $\delta\mathbf{x}$ or $\{\delta\mathbf{x}_i\}$ will denote a vector describing an observable $\delta\mathbf{x}$, and the notation $[\mathbf{F}]_{m \times m}$ and $[k]_{a,b}$ will denote a matrix or submatrix, respectively. Typically, the submatrix $[k]_{a,b}$ will be a 3×3 matrix element of a larger system matrix detailing the interaction of object a with object b in the three spatial dimensions.

To estimate the cluster–cluster stiffness (the restoring force induced in response to a displacement), we calculate the static equilibrium displacement when a force is applied to one cluster center while the other is held fixed. This is done by first projecting out the partitioned Hessian matrix (PHM) of all of the atoms that interact in the region between the cluster centers of (α, β) (Figure 3). (Here the cluster centers are taken to be the α -carbons within each cluster.) The static equilibrium properties of the network must be computed using the Cartesian (non-mass-weighted) stiffness matrix elements for each atom–atom interaction.²⁴ The Cartesian stiffness matrix of interactions between each pair of the set of m atoms will be calculated from the (Amber²²) mass-weighted Hessian by unmass-weighting the latter:

$$[ka]_{i,j}^{(c)} = [ka]_{i,j}^{(m)} m_i^{1/2} m_j^{1/2} \quad (1)$$

Here the superscript (c) refers to the Cartesian force submatrix and the superscript (m) refers to the mass-weighted force submatrix. Each $[ka]_{i,j}^{(c)} [ka]_{i,j}^{(m)}$, is a 3×3 stiffness submatrix corresponding to the interaction of atoms i and j obtained from the Amber Hessian.

The Cartesian cluster–cluster PHM implicitly contains the interaction, $[kp]_{i,j}^{(c)}$, of each pair of atoms in the region between the two α -carbon-based cluster centers of (α, β) (Figure 3). The concerted set of atom–atom interactions within this spring network induces the cluster-to-cluster interaction matrix. (The nodes of interest in this spring model are the α -carbons of the cluster pair, and the goal is to figure out the effective spring constant of the spring network that couple the two α -carbons of the cluster pair.) Here the off-diagonal, $[kp]_{i,j}^{(c)} : i \neq j$, elements of this PHM are the Cartesian stiffness matrix elements of each of the interacting atoms and are projected from the Amber Hessian matrix elements $[ka]_{i,j}^{(c)}$. To ensure that there are six zero-energy rigid displacements for this isolated subsystem of m atoms,²⁵ the diagonal components for the partitioned interaction of the atoms between cluster α and cluster β must then be set according to:

$$[kp]_{i,j}^{(c)} = -\sum_{j \neq i} [kp]_{i,j}^{(c)} \mid i, j \in \{1 \dots m\} \quad (2)$$

For convenience, the m atoms in the interaction network partition are renumbered so that the 1st is the α -carbon of α and the m th is the α -carbon of β . The remaining atoms are ordered arbitrarily and occupy the intervening space (Figure 3) and act as a connected network of springs (Figure 2) that will, as a group, induce the quasi-static reaction in response to the displacement of the m th atom (an α -carbon) while the 1st atom (the other α -carbon) is held fixed. These stiffness submatrices, $[kp]_{i,j}^{(c)}$, are then assembled into the PHM force constant matrix $\mathbf{PH}^{\alpha, \beta}$ (between cluster centers α, β) using:

$$[\mathbf{PH}^{\alpha, \beta}]_{m \times m}^{(c)} \Big|_{i,j} = [kp]_{i,j}^{(c)} \mid i, j \in \{1 \dots m\} \quad (3)$$

Under static loading conditions, the net forces on each of the intervening atoms will be zero. This interaction between the cluster centers and the network of intervening atoms within the partition (i.e., between the centers of α and β) can then be formulated as a $3m$ dof statics problem²⁶ as:

$$\{\delta f_i\}^{(c)} = [\mathbf{PH}^{\alpha, \beta}]_{m \times m}^{(c)} \{\delta x_j\}^{(c)} \quad (4)$$

Here $\{\delta x_j\}^{(c)}$ is a $3m$ dimensional vector composed of 3D 3×1 displacement subvectors δx_j associated with each of the atoms j

$= 1 \dots m$ in the network defined above. Similarly, $\{\delta f_i\}^{(c)}$ is a $3m$ dimensional vector composed of 3D 3×1 induced force subvectors δf_i associated with each of the atoms $i = 1 \dots m$ in this network.

The following boundary conditions apply in this quasi-static regime:

$$\begin{aligned} \delta f_i^{(c)} &= 0: i \in \{2 \dots m-1\} \\ \delta x_1 &= 0 \end{aligned} \quad (5)$$

Because atom 1 is restrained, we can drop it from the system (by removing row 1 and column 1) to obtain the reduced $[\mathbf{PHr}_{ij}^{\alpha, \beta}]_{m-1 \times m-1}^{(c)}$ system:

$$\{\tilde{\delta f}_i\}^{(c)} = [\mathbf{PHr}_{i,j}^{\alpha, \beta}]_{m-1 \times m-1}^{(c)} \{\tilde{\delta x}_j\}^{(c)} \quad (6)$$

Here $\{\tilde{\delta x}_j\}^{(c)}$ is a $3(m-1)$ dimensional vector composed of 3D 3×1 displacement subvectors δx_j associated with each of the atoms $j = 2 \dots m$ in the relevant network of atoms (again, the displacement coordinates of atom 1 have been deleted from the overall displacement vector) and analogously for $\{\tilde{\delta f}_i\}^{(c)}$.

To solve this system for the induced displacements, we compute the inverse of this PHM subject to the forces applied on the cluster centers:

$$\{\tilde{\delta x}_j\}^{(c)} = [[\mathbf{PHr}_{i,j}^{\alpha, \beta}]_{m-1 \times m-1}^{(c)}]^{-1} \{\tilde{\delta f}_i\}^{(c)} \quad (7)$$

Each column of the inverse matrix is the (vector) displacement of the $m-1$ atoms (since atom 1 is fixed) in response to applying a unit force on atom_i. The inverse of the effective Cartesian force submatrix between the two cluster centers (α, β) will then be the $(m-1, m-1)$ th 3×3 submatrix element of the inverted PHM matrix $[\mathbf{PHr}_{ij}^{\alpha, \beta}]$:

$$[kc]_{\alpha, \beta}^{-1} = [[\mathbf{PHr}_{i,j}^{\alpha, \beta}]_{m-1 \times m-1}^{(c)}]^{-1} \Big|_{(m-1, m-1)} \quad (8)$$

The inverse of this term, $[kc]_{\alpha, \beta}$, will represent the effective stiffness submatrix for the interaction between the cluster centers of α, β .

One-Dimensional Example. To illustrate the calculation of the effective stiffness matrix constant, we construct a simple example of four atoms in a 1D collinear arrangement. (In this case, the output of the calculation will be a single positive number, that is, the effective force constant governing the stretching of mass 4 when mass 1 is pinned, and the connecting particles, 2 and 3, adjust instantaneously to maintain mechanical equilibrium.) The stiffness matrix for this simple system (presuming unit force constants that connect adjacent atoms) is:

$$\begin{bmatrix} 1 & -1 & 0 & 0 \\ -1 & 2 & -1 & 0 \\ 0 & -1 & 2 & -1 \\ 0 & 0 & -1 & 1 \end{bmatrix} \quad (9)$$

Removing the fixed atom 1 (row 1 and column 1) from this system yields the 3×3 matrix:

$$\begin{bmatrix} 2 & -1 & 0 \\ -1 & 2 & -1 \\ 0 & -1 & 1 \end{bmatrix} \quad (10)$$

which has the inverse:

$$\begin{bmatrix} 1 & 1 & 1 \\ 1 & 2 & 2 \\ 1 & 2 & 3 \end{bmatrix} \quad (11)$$

The third column $[1 \ 2 \ 3]^T$, is the displacement of atoms 2–4 in response to a unit force on atom 4. In this 1D system, the aggregate stiffness through this group of three springs will therefore be the scalar $\delta f_3/\delta x_3 = 1/3$, or 0.3333. This result coincides with the net stiffness through three springs, having unit force constants, arranged in series.²⁶

Cluster–Cluster Interaction. Returning to the case of a protein moving in 3D, the pairwise interaction between the two CG clusters is modeled as two point masses connected by a spring. To build the molecular level, we need to estimate the cluster-based force matrix, the effective 3×3 stiffness submatrix elements between each cluster. This interaction can be approximated as a rank-one matrix between the cluster centers (i.e., between the α -carbons). The effective force constant, $\kappa_{\alpha,\beta}$ of this spring is extracted from the data in the submatrix element obtained from eq 8 by diagonalizing the inverse of this 3×3 matrix and using the eigenvalues to approximate the force constant along the three principal directions. The dominant eigenvector is expected to occur at or near the direction of the relative displacement between the cluster centers. If this condition holds and the other two eigenvalues are small in comparison, the rank-one approximation will be nearly exact. In fact, in our analysis, we found that the lesser two eigenvalues were consistently small in comparison with the largest eigenvalue (which was always positive) and that the dominant eigenvector was close in direction to the relative displacement vector between the two cluster centers. Now, if we calculate $[kc]_{\alpha,\beta}$ (obtained by inverting $[kc]_{\alpha,\beta}^{-1}$), we obtain the force constant as:

$$\kappa_{\alpha,\beta} = \max(\lambda_k) \quad (12)$$

with λ_k being the largest eigenvalue of $[kc]_{\alpha,\beta}$.

Using this force constant, the rank-one stiffness submatrix element between clusters α,β can then be estimated using the outer product formula:

$$[k]_{\alpha,\beta}^{(c)} = \kappa_{\alpha,\beta} \frac{(\mathbf{r}_\beta - \mathbf{r}_\alpha) \otimes (\mathbf{r}_\beta - \mathbf{r}_\alpha)}{\|\mathbf{r}_\beta - \mathbf{r}_\alpha\|^2} \Big|_{\alpha \neq \beta} \quad (13)$$

where \otimes indicates the dyadic or outer product and $(\mathbf{r}_\beta - \mathbf{r}_\alpha)$ is the relative equilibrium displacement between cluster centers α and β .

Finally, once each of the L 3×3 cross-cluster stiffness submatrix elements, $k_{\alpha,\beta}$, have been estimated (eq 13 above); they are plugged into the down-sampled, $L \times L$, cluster-based molecular Hessian as the off-diagonal cluster-to-cluster interaction terms. One can now assemble the Cartesian, molecule level, flexible-cluster-based force constant matrix as:

$$[\mathbf{F}_{fc}]_{L \times L}^{(c)} \Big|_{(\alpha,\beta)} = \begin{cases} -[k]_{\alpha,\beta}^{(c)}, & \alpha \neq \beta \\ \sum_{\alpha \neq \beta} [k]_{\alpha,\beta}^{(c)}, & \alpha = \beta \end{cases} \quad \alpha, \beta \in \{1 \dots L\} \quad (14)$$

Note that the on-diagonal submatrices ($\alpha = \beta$) are constructed from the off-diagonal matrices ($\alpha \neq \beta$) so as to ensure that there are six zero-energy rigid displacements of the overall molecule.²⁵

Calculation of Flexible Cluster Friction Matrix. The atom level friction matrix $[\Gamma_a]_{N \times N}$ is computed from¹⁰ as:

$$[\Gamma_a]_{N \times N} = [[\gamma]_{i,i}]_{N \times N} \quad (15)$$

Here the atomic friction, $\gamma_{i,i}$ is a 3×3 submatrix element given by the formula:^{10,27}

$$[\gamma]_{i,i} = 6\pi\eta a_i [\mathbf{I}]_{3 \times 3}, \quad 1 \leq i \leq N \quad (16)$$

where η is the solvent viscosity (chosen in our numerical calculations below to be 1 cP, the viscosity of water). Furthermore, a_i is the hydrodynamic radius of $atom_i$ determined by calculating the solvent-accessible surface area (SASA)^{8,10,27} of this atom and $[\mathbf{I}]_{3 \times 3}$ is the 3×3 identity matrix. The notation of eq 15 indicates that the 3×3 friction submatrices for each atom are inserted as the diagonal “elements” of the $3N \times 3N$ matrix that contains the atomic friction constants of each dof of the relevant N -atom system.

In the fg cluster formulation, the effective linear projection operator¹⁰ has only a translational component. This is not unreasonable because the close-packing and stiff covalent links between many pairs of clusters, particularly along the backbone, tend to limit the rotation of the clusters within the context of a compact folded protein domain.

To calculate the fc friction matrix for this simplified case, one simply adds the atom level friction coefficient from each of the atoms in a given (single amino acid) cluster α to give the friction elements of the *diagonal* cluster friction matrix:

$$[\gamma]_{\alpha,\alpha} = \sum_{i \in \{\alpha\}} [\gamma]_{i,i} \quad (17)$$

The equations of motion for overdamped Langevin dynamics (noted below) require the friction matrix to be invertible. The all-atom friction matrix $[\Gamma_a]_{N \times N}$ will actually be noninvertible if some atoms in the system have zero SASA. This scenario will occur for larger compact proteins in which the interior is not accessible to the solvent. To accommodate this situation, one can assign a small but finite friction to the zero-valued elements. If a value of 10^{-5} times the largest external friction coefficient is assigned to these elements, the matrix can be inverted and the propagator matrix can be computed. We also note that in our numerical calculations (detailed below), varying the range of values from (10^{-2} to 10^{-10}) had minimal impact on the resultant relaxation dynamics. With this modification to the all-atom friction matrix and applying the projection operator, the CG fc diagonal friction matrix is computed from the cluster friction elements by:

$$[\Gamma_{fc}]_{L \times L}^{(c)} = [[\gamma]_{\alpha,\alpha}]_{L \times L} \quad (18)$$

Again, the 3×3 submatrices for each C_α atom are packed along the diagonal elements of the $3L \times 3L$ matrix that contains the friction constants for each dof in the final C_α representation of the protein.

Flexible Cluster Formulation within the Overdamped Limit. The dynamic formulation for the overdamped fc system is similar to the all-atom version. The appropriate time evolution is prescribed by the Smoluchowski equation for motion on a multidimensional quadratic PES. In particular, the time-dependent expectation values of the displacement coordinates $\delta q_L^{(c)}(t)$ obey the following equation of motion, independent of the system temperature:^{10,28,29}

$$[\Gamma_{fc}]_{L \times L}^{(c)} \delta \dot{q}_L^{(c)}(t) = -[\mathbf{F}_{fc}]_{L \times L}^{(c)} \delta q_L^{(c)}(t) \quad (19)$$

Here the matrices $[\Gamma_{fc}]_{L \times L}$ and $[\mathbf{F}_{fc}]_{L \times L}$ are the fc friction matrix and the fc force matrix, computed according to the down-sampling protocol given above. This system has the solution:

$$\delta\mathbf{q}_t^{(c)} = \exp(-[\mathbf{A}_{fc}]_{L \times L}^{(c)} t) \delta\mathbf{q}_0^{(c)} \quad (20)$$

where

$$[\mathbf{A}_{fc}]_{L \times L}^{(c)} = [\Gamma_{fc}]_{L \times L}^{-1}^{(c)} [\mathbf{F}_{fc}]_{L \times L}^{(c)} \quad (21)$$

and $\delta\mathbf{q}_0^{(c)}$ is the vector of initial displacements (dropping the L subscript on displacement coordinate vectors for notational simplicity).

For practical computational reasons, it is useful to perform the simple coordinate scaling transformation:

$$\delta\mathbf{q}' = [\Gamma_{fc}]_{L \times L}^{-1/2}^{(c)} \delta\mathbf{q} \quad (22)$$

One then obtains the *symmetric* friction weighted Hessian matrix used to determine the overdamped modes of the system:

$$\mathbf{A}' = [\mathbf{F}_{od}]_{L \times L} = [\Gamma_{fc}]_{L \times L}^{-1/2}^{(c)} [\mathbf{F}_{fc}]_{L \times L}^{(c)} [\Gamma_{fc}]_{L \times L}^{-1/2}^{(c)} \quad (23)$$

and the associated time evolution equation:

$$\delta\dot{\mathbf{q}}'(t) = -[\mathbf{F}_{od}]_{L \times L} \delta\mathbf{q}'(t) \quad (24)$$

which has the solution:

$$\delta\mathbf{q}'(t) = \exp(-\mathbf{A}' t) \delta\mathbf{q}_0' \quad (25)$$

SECTION 3: MOLECULAR SYSTEMS

The dynamic problem we study here is the relaxation of a specified globular ligand binding protein to the apo state after the ligand dissociates from the holo state. In this instance, the holo state is simulated by applying a force sufficient to induce the holo conformation within the harmonic energy landscape of the apo state.²⁹

Nonequilibrium Response Calculation. The response to ligand dissociation was simulated by applying the displacement needed to induce the bound state and then following the ensuing relaxation. The energy-minimized open structure, illustrated for FBP in Figure 4, was used to calculate the Hessian for the harmonic PES, and the minimized closed state

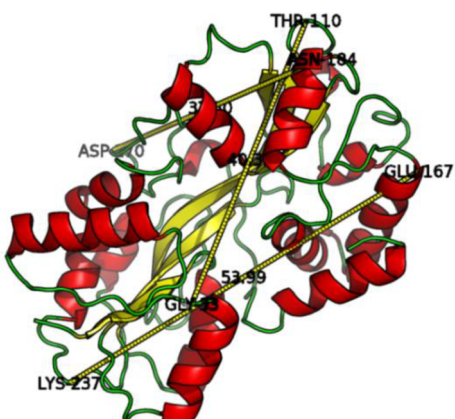


Figure 4. Ferric binding protein [PDB: 1DV9] shown in the open (unliganded) conformation. The tagged residue pairs used to report distance relaxation are labeled. This *unbound* state was used to calculate the harmonic potential energy surface (PES). (This Figure appeared in ref 10 and is reproduced here for convenience.)

(along with the open state) was used to calculate the initial perturbation (atomic displacements relative to their equilibrium values in the open-state conformation). These components, combined within the context of the fc overdamped Langevin (Smoluchowski) framework, were used to generate a trajectory in response to ligand dissociation. The system matrix was processed and propagated in time for >2 ns. Conformations (given in terms of Cartesian displacements) were produced every 1/20 ps and used to calculate the progress of tagged-residue distances. The propagation equations were processed using the linear algebra modules within LAPACK/BLAS.

Potential Energy Surface Calculation. The minimized open state of FBP was prepared from the (unbound) X-ray structure (PDB: 1DV9) by conjugate gradient minimization to a gradient RMS value of 10^{-8} kcal/(Å·mol) in gas phase using AMBER-10. This minimized structure was then used to calculate the all-atom Hessian matrix that prescribes the harmonic energy basin in the neighborhood of the minimum. Similarly, the D chain of PDB structure 150L was used to compute the minimized open state of T4 lysozyme.

The Hessian was derived by minimization of the crystal structure in the gas phase using a standard all-atom empirical force field. The resulting minimized structure was similar in shape and topology to the crystal structure. This approach was taken to enable a (critical) direct comparison with the RTB-dynamics results presented in a recent publication.¹⁰ Solvation effects will modify the Hessian matrix elements, but the overall effect will be similar to the gas phase results.³⁰ Specifically, the interaction of the protein with the surrounding water molecules will likely lead to confinement of the protein atoms and result in steeper potential energy wells.³⁰ Including these effects is not expected to significantly change the quantitative details of the results, particularly in regards to the accuracy of the FC method with respect to the all-atom control system.

Initial Perturbation. The initial displacement of FBP was calculated from the difference between the liganded (PDB: 1MRP) and the unliganded (PDB: 1DV9) states. To minimize any excessive strain energy in the closed (liganded) state, we minimized the closed state to 10^{-3} kcal/(Å·mol) using AMBER-10, and it was subsequently aligned using the align module within the Pymol molecular modeling system.³¹ The initial nonequilibrium perturbation was computed as: $\delta\mathbf{x}^{\text{initial}} = \mathbf{x}^{\text{holo}} - \mathbf{x}^{\text{apo}}$. Similarly, the liganded state used for the closed state of the T4 lysozyme system was PDB structure 2LZM.

SECTION 4: DISTANCE RELAXATIONS AND MOLECULAR MOTIONS

To characterize the dynamics of these systems and assess the reliability of the method, we monitored the time evolution of the separation distance between $C\alpha$ atoms of select amino acid pairs over the course of the relaxation from the holo to the apo configurations of a protein. In particular, the fc dynamics of two medium sized globular proteins, FBP and T4L, both of which we have studied previously at the all-atom level^{10,29} was computed.

Figure 4 illustrates the three amino acid (AA) pairs in FBP, namely, [E167, K237], [G33, T110], and [N184, D270], which were selected for distance monitoring. Three analogous pairs, namely, [E22, R137], [R52, A160], [S38, K135], where chosen in the T4L protein. For both systems, the shape and time scale of the distance relaxation of the clustered versus nonclustered instances agree very well (see Figures 5 and 6). In both systems, the fc relaxation was slightly faster than the all-atom

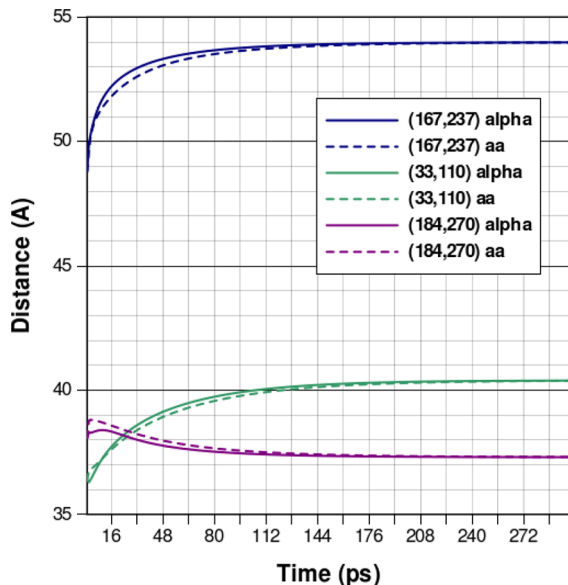


Figure 5. Temporal relaxation of α -carbon pairs [E167, K237], [G33, T110], and [N184, D270] within FBP. For each pair (see Figure legend), the solid line shows the result of the fg cluster model analysis, while the dashed line shows the all-atom analogue.

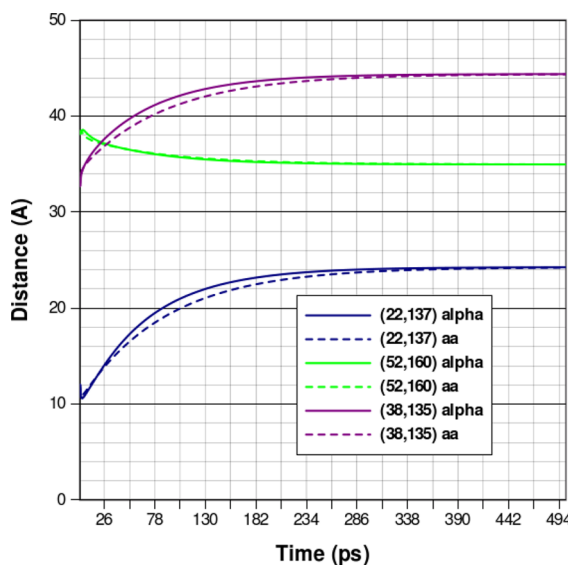


Figure 6. Temporal relaxation of α -carbon pairs [E22, R137], [R52, A160], [S38, K135] within T4L. For each pair (see Figure legend), the solid line shows the result of the fg cluster model analysis, while the dashed line shows the all-atom analogue.

(nonclustered) control. For the FBP system, it is instructive to compare the AA distance relaxation curves shown in Figure 5 with the corresponding results obtained using the standard RTB approximation (Figures 5–7 of ref 10). The RTB approximation using single residue blocks generates responses that are ca. four times faster than the analogous *fc* approximation calculation.¹⁰ The latter approximation tracks the exact all-atom dynamics of the system quite faithfully because it eliminates the artificial stiffening of interblock (or intercluster) interactions induced by the RTB procedure.

We also analyzed the BrMs (Brownian modes, i.e., the eigenvectors of the friction weighted effective Hessian matrix in eq 23) for both protein systems. In particular, we observed that

the initial displacement vector characterizing each protein could be decomposed as a linear combination of two dominant “vibrational” eigenvectors (i.e., motions that correspond to internal deformation of the protein rather than overall translations or rotations). The most dominant BrM in each protein system (see Figures 7 and 8) corresponds to a cleft-

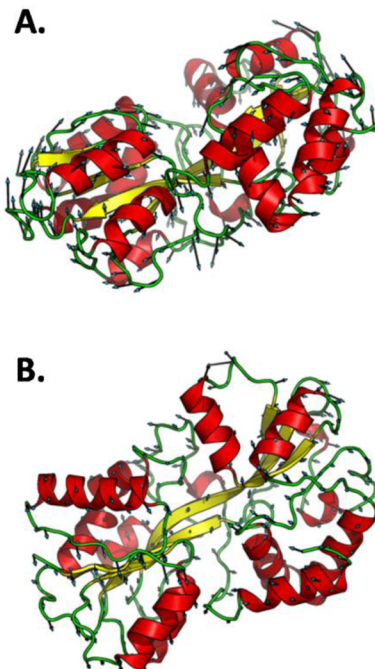


Figure 7. Two highest projecting nontrivial overdamped BrMs within FBP. (A) Cleft-opening mode. (B) Cleft-positioning mode.

opening motion, which is consistent with the major movement due to the presence of the ligand in the induced fit binding

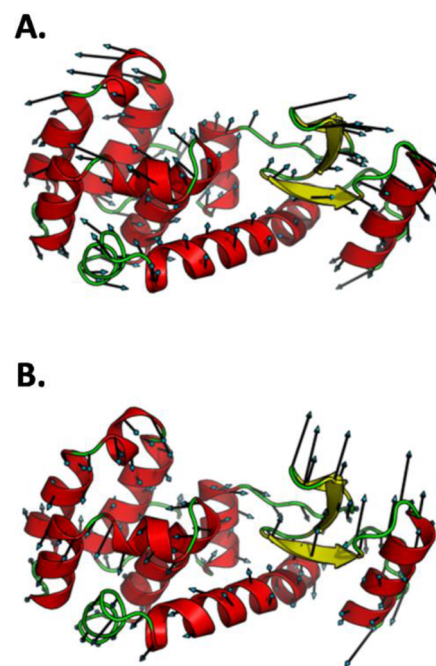


Figure 8. Two highest projecting nontrivial BrMs within T4 lysozyme. (A) Cleft-opening mode. (B) Cleft-positioning mode.

model.³² The second most dominant BrM (see Figures 7 and 8) represents an alignment movement needed to achieve optimal fit of the ligand. This latter mode is also consistent with an induced fit hypothesis.³²

■ SECTION 5: DISCUSSION

Reduction in Computational Complexity. To appreciate the reduction in complexity achieved by the *fc* method, we formulate the processing time complexity in terms of the CG cluster size. If a system of na atoms is diagonalized, its time complexity is na^3 . If the cluster size is 10 (about the size of a small amino acid) the complexity reduces to:

$$\left(\frac{na}{10}\right)^3 = \frac{na^3}{1000} \quad (26)$$

For a system having na atoms, the number of pairwise interactions can be approximated as:

$$\frac{\left(\frac{na}{10}\right)\left(\frac{na}{10}-1\right)}{2} \quad (27)$$

For a cluster size of 10, the number of operations needed to calculate the pairwise cluster–cluster stiffness is $\sim(2 \times 10)^3$. (This third-order relationship relates the size of a system to the number of operations needed to find the eigenvectors of that system.) To find the break-even point in terms of the number of atoms in the molecule where the divide-and-conquer strategy employed in the *fc* method becomes favored, we solve the equation:

$$\begin{aligned} & \underbrace{\frac{\left(\frac{na}{10}\right)\left(\frac{na}{10}-1\right)}{2}}_{\text{number pairs}} \underbrace{(2 \cdot 10)^3}_{\text{complexity per pair}} + \underbrace{\left(\frac{na}{10}\right)^3}_{\text{diagonalizing coarse grain system}} = \underbrace{na^3}_{\text{diagonalizing all atom system}}, \\ & na^2 \cdot 40 + \frac{na^3}{1000} = na^3, \\ & na^3(1000 - 1) = na^2 \cdot 40 \cdot 1000, \\ & na^2(na - 40) \approx 0 \end{aligned} \quad (28)$$

This shows that, for a cluster size of ~ 10 , the divide-and-conquer approach becomes favored for $na \geq 40$.

Localized Force Transmission. This formulation tacitly assumes (due to the distance cutoff and localized analysis of stiffness) that the predominant forces driving the relaxation are transmitted locally. The numerical results obtained in our studies of FBP and T4L demonstrate that this assumption is reasonable.

Stokes Law Approximation to Friction. In a previous all-atom MD study,³⁰ the full friction matrix was calculated for carboxymyoglobin, a protein similar in size to those we have considered. The results showed that the off-diagonal elements of the friction matrix increased with temperature and solvation but were small enough for the diagonal approximation to be useful.

In regards to the magnitude of the friction constants of the internal atoms, the results of an MD analysis³⁰ suggested that for the functionally important low-frequency (collective) modes the internal atomic friction constants are nearly a factor of 10 smaller than the external atom friction constants. Using this 10:1 ratio of external to internal friction, we found only minor differences in the relaxation time scales and the shape of the

normal modes as predicted by the *fc* method relative to the corresponding results obtained for the all-atom control system. This small difference suggested that instantaneous mechanical equilibrium of the internal atoms was still established to a reasonable approximation. In the atomistic simulation³⁰ the surface friction was found to be somewhat lower than that estimated using the Stokes approximation for the more collective, low-frequency modes. This analysis also showed that the Stokes approximation overestimated the number of overdamped modes but that the lowest modes in either case (atomistic simulation, Stokes law) were overdamped. Because the relaxation motion in our systems occurred predominantly along the first two nontrivial modes (the modes corresponding to which were found to be overdamped for the similar sized protein analyzed in ref 30), the use of the Stokes law allowed for a valid comparison to our previous results.

Variation in Pairwise Force Constants. Because the interatom force constants are computed using the full AMBER force field, there is significant variation among the atom–atom stiffnesses. This is reflected in the cluster-to-cluster stiffnesses. The cluster–cluster stiffness constants ($\kappa_{\alpha\beta}$) vary over three orders of magnitude. The highest stiffness occurs, not surprisingly, along the peptide backbone (Figure 2A), where the stiffness was on the order 200 kcal/(Å² mol). The next highest occur in areas of loop bending and where hydrogen bonds are formed such as in β strands; here the representative force constant was $\sim(10-50)$ kcal/(Å² mol). Finally, the lowest stiffness occurs in areas having weak van der Waals and long-range electrostatic interactions (Figure 2B), where the characteristic stiffness was $\sim(1-10)$ kcal/(Å² mol).

■ SECTION 6: CONCLUSIONS

Down-sampling the all-atom Hessian yields a reasonable description of the protein dynamics in terms of the slow BrMs. In the overdamped limit (where the high-frequency motion of the protein is rapidly dissipated), the down-sampled force matrix faithfully describes conformational motion down to the residue level. The rapid relaxation of the atoms within the interior region (below the solvent surface) induces a quasi-static equilibrium that can be analyzed using techniques similar to those used in the static analysis of truss systems.²⁶

■ AUTHOR INFORMATION

Corresponding Author

*E-mail: coalson@pitt.edu.

Notes

The authors declare no competing financial interest.

■ ACKNOWLEDGMENTS

We gratefully acknowledge financial support from NSF grant CHE-0750332 and the computational resources of the Center for Molecular and Materials Simulations (CMMS) at the University of Pittsburgh. We thank Dr. Sebnem Essiz Gokhan for numerous helpful discussions.

■ REFERENCES

- (1) Henzler-Wildman, K.; Kern, D. Dynamic Personalities of Proteins. *Nature* 2007, 450, 964–972.
- (2) Ansari, A.; Berendzen, J.; Bowne, S. F.; Frauenfelder, H.; Iben, I. E.; Sauke, T. B.; Shyamsunder, E.; Young, R. D. Protein States and Protein quakes. *Proc. Natl. Acad. Sci. U.S.A.* 1985, 82, 5000–5004.
- (3) Barry, P. H.; Lynch, J. W. Ligand-Gated Channels. *IEEE Trans. Nanobiosci.* 2005, 4, 70–80.

- (4) Sherwood, P.; Brooks, B. R.; Sansom, M. S. P. Multiscale Methods for Macromolecular Simulations. *Curr. Opin. Struct. Biol.* **2008**, *18*, 630–640.
- (5) Tozzini, V. Coarse-Grained Models for Proteins. *Curr. Opin. Struct. Biol.* **2005**, *15*, 144–150.
- (6) Smith, A. V.; Hall, C. K. Assembly of a Tetrameric Alpha-Helical Bundle: Computer Simulations on an Intermediate-Resolution Protein Model. *Proteins: Struct., Funct., Genet.* **2001**, *44*, 376–391.
- (7) Essiz, S.; Coalson, R. D. A Rigid-Body Newtonian Propagation Scheme Based on Instantaneous Decomposition into Rotation and Translation Blocks. *J. Chem. Phys.* **2006**, *124*, 144116:1–11.
- (8) Essiz, S. G.; Coalson, R. D. Langevin Dynamics of Molecules with Internal Rigid Fragments in the Harmonic Regime. *J. Chem. Phys.* **2007**, *127*, 104109-1–104109-14.
- (9) Furois-Corbin, S.; Smith, J.; Kneller, G. Picosecond Timescale Rigid-Helix and Side-Chain Motions in Deoxymyoglobin. *Proteins: Struct., Funct., Genet.* **1993**, *16*, 141–154.
- (10) Manson, A. C.; Coalson, R. D. Response of Rotation–Translation Blocked Proteins Using Langevin Dynamics on a Locally Harmonic Landscape. *J. Phys. Chem. B.* **2012**, *116*, 12142–12158.
- (11) Chun, H. M.; Padilla, C. E.; Chin, D. N.; Watanabe, M.; Karlov, V. I.; Alper, H. E.; Soosaar, K.; Blair, K. B.; Becker, O. M.; Caves, L. S. D.; et al. MBO(N)D: A Multibody Method for Long-Time Molecular Dynamics Simulations. *J. Comput. Chem.* **2000**, *21*, 159–184.
- (12) Hicks, S. D.; Henley, C. L. Coarse-Grained Protein-Protein Stiffnesses and Dynamics from All-Atom Simulations. *Phys. Rev. E* **2010**, *81*, 030903:1–4.
- (13) Moritsugu, K.; Smith, J. C. Coarse-Grained Biomolecular Simulation with REACH: Realistic Extension Algorithm via Covariance Hessian. *Biophys. J.* **2007**, *93*, 3460–3469.
- (14) Yang, L. W.; Rader, A. J.; Liu, X.; Jursa, C. J.; Ching, S. C.; Karimi, H.; Bahar, I. oGNM: Online Computation of Structural Dynamics Using the Gaussian Network Model. *Nucleic Acids Res.* **2006**, *34*, 24–31.
- (15) Ming, D.; Wall, M. E. Quantifying Allosteric Effects in Proteins. *Proteins* **2005**, *59*, 697–707.
- (16) Keramidas, A.; Moorhouse, A. J.; Peter, P. R.; Barry, P. H. Ligand-Gated Ion Channels: Mechanisms Underlying Ion Selectivity. *Prog. Biophys. Mol. Biol.* **2004**, *86*, 161–204.
- (17) Law, R. J.; Henchman, R. H.; McCammon, J. A. Spontaneous Conformational Change and Toxin Binding in $\alpha 7$ Acetylcholine Receptor: Insight into Channel Activation and Inhibition. *Proc. Natl. Acad. Sci. U.S.A.* **2005**, *102*, 6813–6824.
- (18) Cheng, M. H.; Coalson, R. D.; Tang, P. Molecular Dynamics and Brownian Dynamics Investigation of Ion Permeation and Anesthetic Halothane Effects on a Proton-Gated Ion Channel. *J. Am. Chem. Soc.* **2010**, *132*, 16442–16449.
- (19) Simons, J.; Jorgensen, P.; Taylor, H.; Ozment, J. Walking on Potential Energy Surfaces. *J. Phys. Chem.* **1983**, *87*, 2745–2753.
- (20) Ming, D.; Wall, M. E. Allostery in a Coarse-Grained Model of Protein Dynamics. *Phys. Rev. Lett.* **2005**, *95*, 198103-1–198103-4.
- (21) Ermak, D. L.; McCammon, J. A. Brownian Dynamics with Hydrodynamic Interactions. *J. Chem. Phys.* **1978**, *69*, 1352–1360.
- (22) Case, D. A.; Pearlman, D. A.; Caldwell, J. W.; Cheatham, T. E., III; Wang, J.; Ross, W. S.; Simmerling, C. L.; Darden, T. A.; Merz, K. M.; Stanton, R.; et al. AMBER 7; University of California: San Francisco, 2002.
- (23) Preparata, F. P.; Shamos, M. I. *Computational Geometry: An Introduction*; Springer-Verlag: New York, 1988.
- (24) Wilson, E. B.; Decius, J. C.; Cross, P. C. *Molecular Vibrations*; McGraw-Hill: New York, 1955.
- (25) Eckart, C. Some Studies Concerning Rotating Axes and Polyatomic Molecules. *Phys. Rev.* **1935**, *47*, 552–558.
- (26) McGuire, W.; Gallagher, R. H.; Ziemian, R. D. *Matrix Structural Analysis*, 2nd ed.; John Wiley & Sons: New York, 2000.
- (27) Pastor, R. W.; Karplus, M. Parametrization of the Friction Constant for Stochastic Simulations of Polymers. *J. Phys. Chem.* **1988**, *92*, 2636–2641.
- (28) Lamm, G.; Szabo, A. Langevin Modes of Macromolecules. *J. Chem. Phys.* **1986**, *85*, 7334–7348.
- (29) Essiz, S. G.; Coalson, R. D. Dynamic Linear Response Theory for Conformational Relaxation of Proteins. *J. Phys. Chem. B* **2009**, *113*, 10859–10869.
- (30) Moritsugu, K.; Smith, J. Langevin Model of the Temperature and Hydration Dependence of Protein Vibrational Dynamics. *J. Phys. Chem. B* **2005**, *109*, 12182–12194.
- (31) Delano, W. L. *The PyMOL Molecular Graphics System*; Delano Scientific: San Carlos, CA, 2002. <http://www.pymol.org>.
- (32) Koshland, D. Application of a Theory of Enzyme Specificity to Protein Synthesis. *Proc. Natl. Acad. Sci. U.S.A.* **1958**, *44*, 98–104.